Friction and torque govern the relaxation of DNA supercoils by eukaryotic topoisomerase IB

Daniel A. Koster[1], Vincent Croquette[2], Cees Dekker[1], Stewart Shuman[3] & Nynke H. Dekker[1]

[1]*Kavli Institute of Nanoscience, Faculty of Applied Sciences, Delft University of Technology, Lorentzweg 1, 2628 CJ Delft, The Netherlands*
[2]*Laboratoire de Physique Statistique, Ecole Normale Supérieure, 75005 Paris, France*
[3]*Molecular Biology Program, Sloan-Kettering Institute, New York, New York 10021, USA*

Topoisomerases relieve the torsional strain in DNA that is built up during replication and transcription. They are vital for cell proliferation[1–3] and are a target for poisoning by anti-cancer drugs[4,5]. Type IB topoisomerase (TopIB) forms a protein clamp around the DNA duplex[6–8] and creates a transient nick that permits removal of supercoils. Using real-time single-molecule observation, we show that TopIB releases supercoils by a swivel mechanism that involves friction between the rotating DNA and the enzyme cavity: that is, the DNA does not freely rotate. Unlike a nicking enzyme, TopIB does not release all the supercoils at once, but it typically does so in multiple steps. The number of supercoils removed per step follows an exponential distribution. The enzyme is found to be torque-sensitive, as the mean number of supercoils per step increases with the torque stored in the DNA. We propose a model for topoisomerization in which the torque drives the DNA rotation over a rugged periodic energy landscape in which the topoisomerase has a small but quantifiable probability to religate the DNA once per turn.

Type IB topoisomerases alter DNA topology by cleaving and rejoining one strand of the DNA duplex[1], and are able to remove both positive and negative supercoils. *In vivo*, TopIB removes positive supercoils generated in advance of the replication fork[9]. Cleavage occurs via a transesterification reaction in which the scissile phosphodiester is attacked by a tyrosine of the enzyme, resulting in the formation of a DNA–(3′-phosphotyrosyl)–enzyme intermediate and the expulsion of a 5′-OH DNA strand. In the rejoining step, the DNA 5′-OH group attacks the covalent intermediate, resulting in expulsion of the active-site tyrosine and restoration of the DNA phosphodiester backbone.

On the basis of structural[10] and kinetic[11] data, a mechanism has been proposed for TopIB, whereby supercoils are relaxed by swivelling of the DNA about the phosphodiester opposite the nick (Fig. 1a–c). The clamp-like structure of human TopIB around the DNA duplex suggests that the DNA cannot swivel unhindered, and consequently a 'controlled rotation' model has been proposed[10,11]. The swivel mechanism of TopIB action is in stark contrast to the protein-assisted strand-passage mechanism of type IA and type II topoisomerases, in which there is an obligate step-size of 1 or 2 supercoils removed per cleavage–religation cycle, respectively[12–18].

Our experimental strategy entails anchoring a single, continuous linear double-stranded (ds)DNA molecule between a glass surface and a paramagnetic bead. We use a pair of magnets to apply a stretching force F and a degree of supercoiling σ by translating a pair of magnets in the vertical direction or rotating them about their axis, respectively[19]. The height of the bead from the surface is equal to the extension of the DNA molecule. Figure 1d plots the DNA extension as a function of force and torque. In a typical measurement, the DNA molecule is prepared in a positively supercoiled state ($\sigma > 0$), which corresponds to a short extension.

When vaccinia TopIB, a prototypical eukaryotic type IB topoisomerase, is added, we observe discrete, step-wise increases in the extension (Fig. 2a). Each step signifies the removal of DNA supercoils during a single cleavage–religation cycle by a single TopIB enzyme. Using the rotation curve (Fig. 1d), we convert the changes

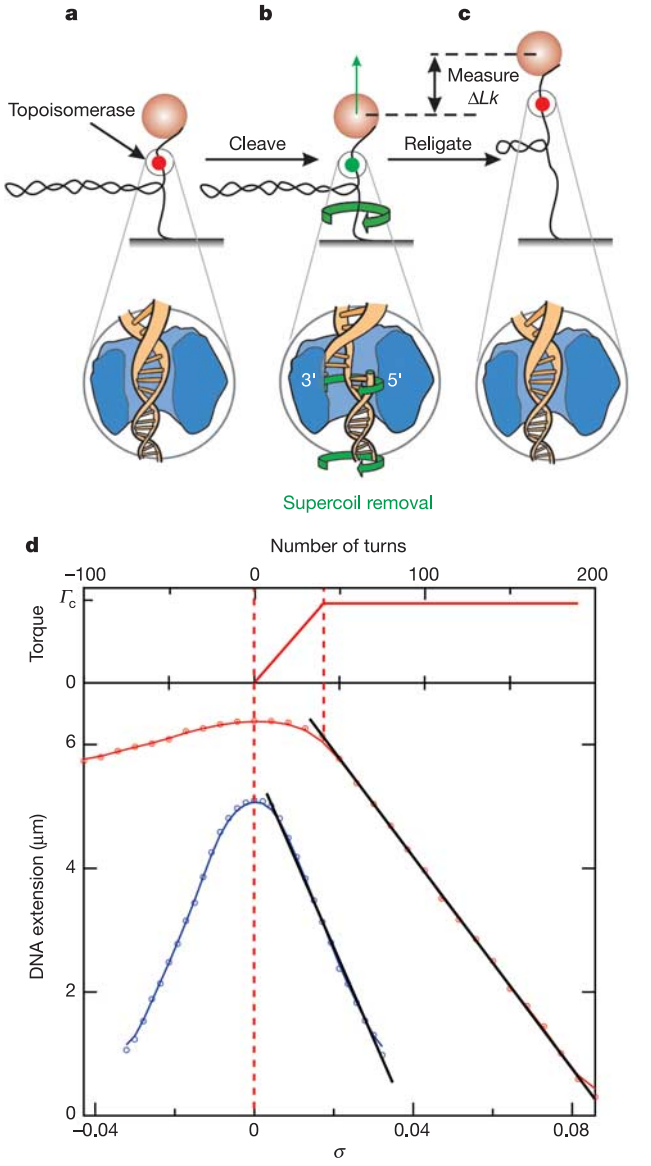

Figure 1 Single-molecule assay for measuring DNA supercoil removal by topoisomerase. **a**, Type 1B topoisomerase is bound non-covalently to a supercoiled DNA molecule. **b**, Topoisomerase establishes a covalent bond to the DNA, creating a nick that allows for rotation of the DNA about the remaining, intact DNA strand (green arrow). In this way, supercoils are removed. **c**, The DNA has been religated by the topoisomerase, terminating the release of supercoils. The height of the bead above the surface has increased, proportional to the number of supercoils removed (ΔLk). **d**, The behaviour of dsDNA under torsion is dependent on the stretching force (data shown for half-length bacteriophage λ DNA). Increasing σ at 1 pN (red curve), the extension initially remains constant and the torque builds up linearly with σ (Twist regime). After a critical buckling torque Γ_c, the torque saturates and the DNA forms plectonemic supercoils. It then contracts linearly with σ (Writhe regime), with a slope of 37 nm per turn (1 pN) and 65 nm per turn (0.2 pN, blue curve). At low stretching force (0.2 pN) the DNA extension is decreased irrespective of the rotation direction as the molecule is supercoiled. At a higher force (1 pN), this occurs only for positive rotations ($\sigma > 0$); at negative rotations, the DNA denatures. Solid coloured lines in rotation curves are splines through experimental data points, black lines are fits to a linear function.

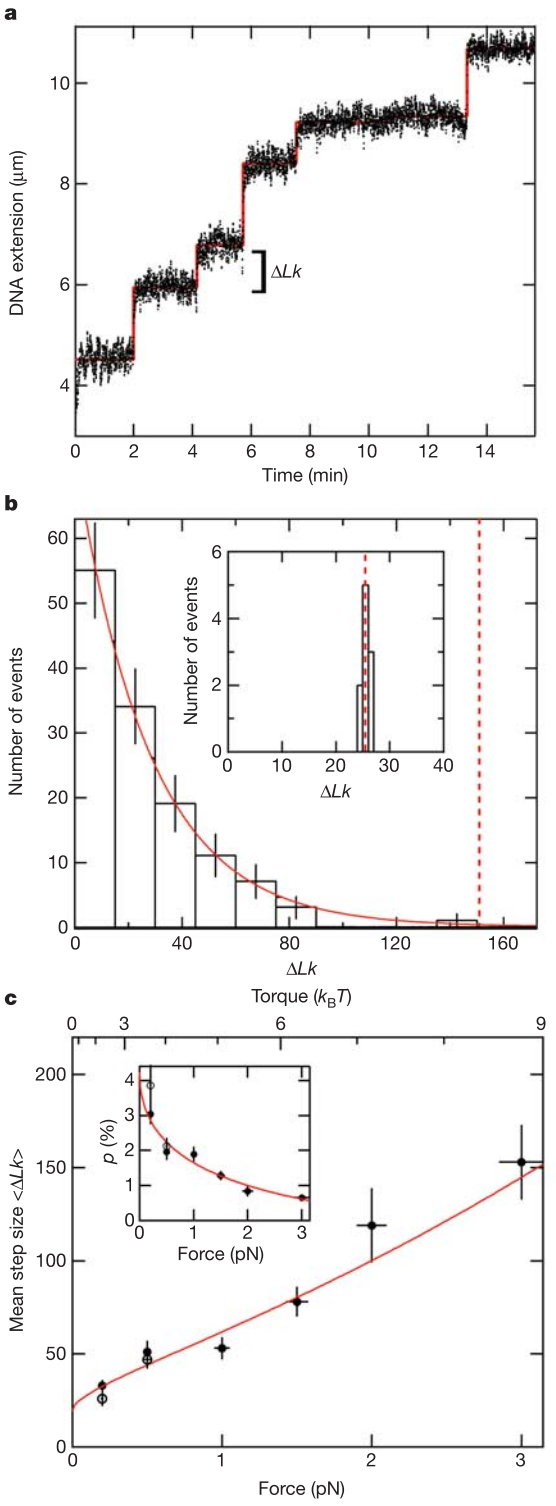

Figure 2 Real-time enzymatic activity and step-size distribution for TopIB acting on a single DNA molecule. **a**, Each time TopIB removes supercoils from the DNA, a step is observed in the DNA extension. **b**, $P(\Delta Lk)$ for TopIB and for nicking enzyme (inset), in units of ΔLk. Vertical dashed red lines show the number of plectonemic supercoils initially incorporated into the DNA. The solid red line is a fit of equation (1) to the data. Error bars denote the square root of the number of events. **c**, $\langle \Delta Lk \rangle$ as a function of applied force and torque. The solid line shows the fit of equation (2) to the data. The inset shows the force-dependence of p (see text). Solid and open circles represent data taken at positive and negative supercoils, respectively.

in DNA extension to a number of rotations removed from the DNA, which equals the change in the linking number ΔLk. The distribution of ΔLk, $P(\Delta Lk)$, has a mean far greater than unity (Fig. 2b) and is well fitted by an exponential (red line in Fig. 2b):

$$P(\Delta Lk) \approx \exp(-\Delta Lk/\langle \Delta Lk \rangle) \quad (1)$$

where $\langle \Delta Lk \rangle$ refers to the mean change in linking number. At higher stretching forces, the functional forms of the distributions are unchanged, but the corresponding values for $\langle \Delta Lk \rangle$ increase significantly (Fig. 2c, solid circles). The functional forms of the distributions are also found to be insensitive to the sign of the supercoiling (data not shown). Within the experimentally accessible regime at negative supercoiling (see Fig. 1d), the values of $\langle \Delta Lk \rangle$ for negative supercoils (Fig. 2c, open circles) are similar to those measured for positive supercoils. In contrast to vaccinia TopIB, a control measurement of $P(\Delta Lk)$ for a nicking enzyme shows a peak that coincides with the number of supercoils initially applied to the DNA molecule (Fig. 2b, inset). Unlike vaccinia TopIB, the nicking enzyme does not possess the ability to religate DNA and therefore all supercoils are released at once.

The exponential functional form of $P(\Delta Lk)$ for vaccinia TopIB can be understood by considering the DNA as it rotates during supercoil release. After nicking of the DNA by transesterification of vaccinia TopIB to the DNA 3′-phosphate end, the DNA rotates inside the enzyme cavity and its 5′-OH end passes the tyrosine-3′-DNA adduct once every turn. At each pass, there is a finite probability p for vaccinia TopIB to religate the DNA and a probability $q \equiv 1 - p$ that the enzyme does not religate the DNA. In accordance with this, the probability distribution for observing steps of size ΔLk is given by the discrete probability function of the geometric distribution[20] $(\Delta Lk = 1, 2, \ldots) : P(\Delta Lk) = pq^{\Delta Lk - 1} = p(1-p)^{\Delta Lk - 1}$, where $\langle \Delta Lk \rangle \equiv 1/p$. The continuum limit of this distribution is equation (1). We find that by increasing the stretch-

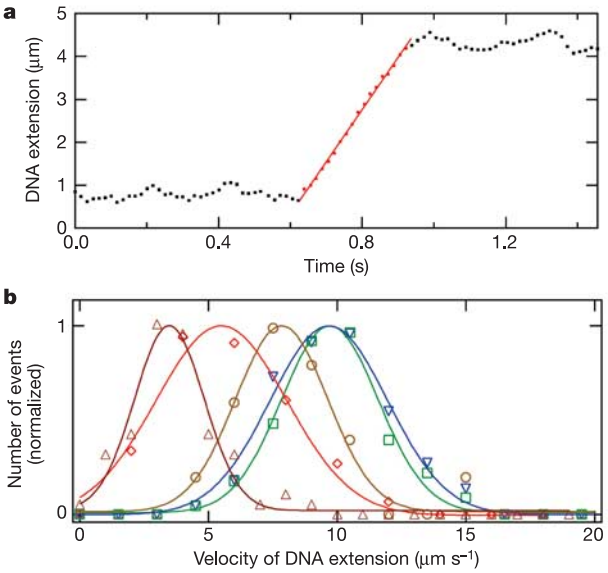

Figure 3 Measurement of velocity of DNA extension during supercoil release. **a**, A step in DNA extension as a consequence of supercoil removal is characterized by a linear increase in DNA extension (red points) and is fitted with a linear function to obtain the rate (solid red line). **b**, Velocity of DNA extension distributions taken at 0.2 pN for human TopIB (dark red triangles, $\langle v \rangle = 4.1 \pm 0.2\,\mu m\,s^{-1}$), wild-type TopIB (red diamonds, $\langle v \rangle = 6.7 \pm 0.2\,\mu m\,s^{-1}$), the TopIB Y70A mutant (beige circles, $\langle v \rangle = 8.9 \pm 0.6\,\mu m\,s^{-1}$), nicking enzyme (blue triangles, $\langle v \rangle = 10.5 \pm 0.2\,\mu m\,s^{-1}$) and for a mix of TopIB mutant Y274F and nicking enzyme (green squares, $\langle v \rangle = 10.5 \pm 0.2\,\mu m\,s^{-1}$). Solid lines are gaussian fits to the data. Means are numerical averages with the corresponding s.e.m.

ing force from 0.2 pN to 3 pN, the probability of religation per turn decreases from 3% to 0.7% (Fig. 2c, inset). Because a strand-passage mechanism implies that $\langle \Delta Lk \rangle$ is independent of the stretching force[17], we conclude that our data are inconsistent with such a model. Our results are, however, fully consistent with a swivel mechanism.

We are able to resolve in real-time the velocity of DNA extension during supercoil removal. We measure this both for vaccinia TopIB and for endonucleolytic cleavage of one strand by nicking enzymes (Fig. 3). The velocity value is a measure of the rate at which the DNA swivels in the topoisomerase cavity as the supercoils are released. The data in Fig. 3b clearly show that vaccinia TopIB (red diamonds) slows down the DNA rotation rate compared to the unhindered rate observed for the nicking enzymes (blue triangles). Control experiments with two different vaccinia TopIB mutants and with human TopIB provide further evidence that the decreased rotation rate in the TopIB reaction is caused by friction between the topoisomerase and the rotating DNA. First, we excluded the possibility that multiple topoisomerases bound to the DNA at sites other than the cleavage site were interacting with each other[21] in a manner that caused a decreased rotation rate. This was accomplished by a mixing experiment in which the nicking enzyme was reacted with the DNA in the presence of the vaccinia TopIB active-site mutant Y274F (green squares), which binds DNA noncovalently but is incapable of transesterification[22]. The rotation rate observed in the mixed reaction was indistinguishable from the rate observed with the nicking enzyme only. Second, we measured the effect of the vaccinia Y70A mutation on the DNA rotation rate. Tyr 70 is located on the concave surface of the amino-terminal domain of vaccinia TopIB, which clamps over the DNA duplex in the major groove on the helical face opposite the scissile phosphodiester[23]. Owing to the loss of this amino-acid side chain lining the protein–DNA interface, we observe an increase in the DNA rotation rate (beige circles) compared with wild-type vaccinia TopIB. Extending these measurements to human TopIB (dark red triangles), we find that the DNA rotation rate is lower than for wild-type vaccinia TopIB. Human TopIB encircles the DNA duplex fully[7], but vaccinia TopIB has the form of a C-shaped clamp[6,8]. Accordingly, human TopIB presumably offers less freedom for the DNA to rotate than vaccinia TopIB. These data provide what is, to our knowledge, the first direct measurement of friction[24,25] in the TopIB relaxation mechanism.

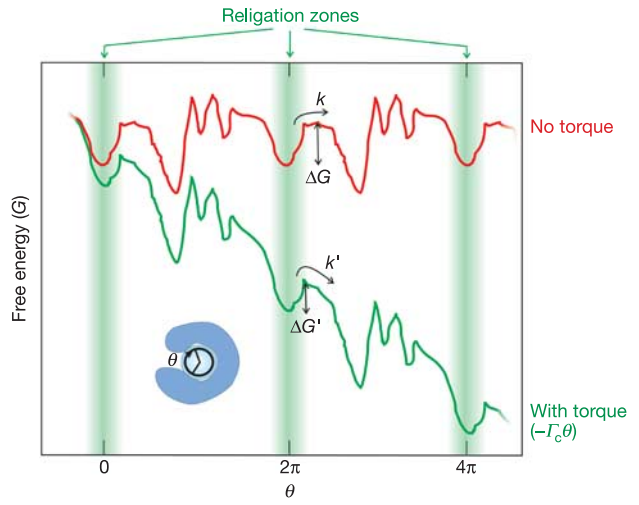

Figure 4 Schematic description of the model. The free energy associated with the angle of rotation between the 5′-OH end of the noncovalently held strand and the tyrosine-3′–DNA adduct in the absence (red curve) and presence (green curve) of torque in the DNA. The effect of the torque is to tilt the landscape, decreasing the barrier height ΔG to $\Delta G'$. This increases the escape rate k to k' from the well in which the rate of religation is maximal. This effectively decreases the religation probability per turn (see text).

We propose a model that describes the effect of friction and torque on enzymatic activity. Our model has three ingredients. First, the rotation of the DNA inside the enzyme clamp is not free but is hindered by friction, as indicated by our velocity measurements. This is modelled by a random walk over a rugged free-energy landscape (Fig. 4), with the rotation angle θ between the 5′-OH end of the noncovalently held strand and the tyrosine-3′–DNA adduct as the reaction coordinate. The DNA rotation is not smoothly continuous, but the free energy profile and accordingly the rotation rate vary during a single rotation. This variability in rotation speed could stem from the notion that the cross-sectional size of the DNA at the nick changes dramatically, from 2 nm at $\theta = 0$ to about 4 nm at $\theta = 180°$. We make no assumptions about the exact shape of the energy landscape. The rate k across each of the barriers with height ΔG in this landscape follows an Arrhenius relation, $k \approx \exp(-\Delta G/k_B T)$, where k_B is the Boltzmann constant and T the temperature in Kelvin.

Second, the mechanically applied constant torque Γ_c drives the uncoiling. It is modelled by tilting the entire energy landscape by $-\Gamma_c\theta$. This decreases ΔG by an amount $\Gamma_c\delta\theta$, where $\delta\theta$ is the angle from the well to the transition state. The rate k' in the presence of a torque Γ_c thus becomes: $k' \approx \exp(-\Delta G'/k_B T) = \exp(-(\Delta G - \Gamma_c\delta\theta)/k_B T)$. The force-dependence of Γ_c is given by[26] $\Gamma_c(F) = \sqrt{2k_B T\xi F}$, where ξ is the bending persistence length of a dsDNA molecule[27] ($\xi = 53 \pm 2$ nm).

Third, within each 2π rotation of the DNA inside the topoisomerase cavity, there is only one position with a significant probability to religate the DNA. This is reasonable because the rotating 5′-OH end needs to be in close proximity (on the order of a few ångströms) to the DNA–3′-phosphotyrosine adduct before a religation can occur. At this position in the energy landscape, there is a possibility of establishing a covalent bond, with rate k_r. The religation probability per turn p is thus given by $p = T_{res}k_r = k_r/k'$, where $T_{res} \equiv 1/k'$ is defined as the residence time in the well at the religation location. As a function of torque, and thus force, we deduce that $p(F) \approx \exp(-\Gamma_c\delta\theta/k_B T) = \exp(-\delta\theta\sqrt{2\xi F/k_B T})$ or,

$$\langle \Delta Lk(F) \rangle = \langle \Delta Lk \rangle_{F=0} e^{\delta\theta\sqrt{2\xi F/k_B T}} \quad (2)$$

Equation (2) provides a good fit of the data for $\langle \Delta Lk \rangle$ versus force (red line in Fig. 2c). We conclude that our model provides a good description of the single-molecule data at positive supercoils. We obtain an estimate for $\delta\theta$ of 0.23 ± 0.02 radians (13°) and an estimate for $\Delta Lk_{F=0}$ of 19.3 ± 2.3 supercoils per cycle. These numerical values might be specific to the removal of positive (rather than negative) supercoils.

Bulk measurements previously performed on plasmids containing 15 ± 2 supercoils yielded an average number of supercoils removed per cleavage–religation cycle of 5 ± 1.5 (ref. 11). This value was indirectly obtained using ensemble-averaged rate constants, whereas our experiment directly measures the number of removed supercoils. In addition, the low initial number of supercoils applied in the plasmid (roughly an order of magnitude lower than in our measurements) may have restricted the observation of large numbers of supercoils removed per cleavage–religation cycle. This could have biased the average number of supercoils released in bulk towards lower values.

An alternative model could consider the stretching force F applied to the DNA, rather than torque, as the parameter governing the religation probability. In such a model, the enzyme would have to perform work over a distance δx against F to religate the DNA. Fitting such a force-dependent model to our data yields the very large value of 20 Å for the force-sensitive step δx. However, earlier work[28] showed that although vaccinia TopIB can religate 5′-OH DNA across a one-nucleotide gap (a distance roughly 3 Å larger than a nick), the religation rate for this reaction is already decreased by a

factor of 200 in comparison to the religation rate across a nick. It thus seems unrealistic that any religation events would be observed with a separation of 20 Å. Accordingly, we do not favour such a force-dependent mechanism. □

Methods

Enzymes and buffers

Wild-type and mutant vaccinia TopIB proteins were purified as described previously[29]. Nicking enzymes N.BbvCIA, N.BbvCIB and N.BstNBI were purchased from New England Biolabs. Human TopIB (100 kDa fragment) was purchased from Topogen. The step-size distributions were measured in buffer containing 10 mM Tris-HCl pH 8.0, 50 mM NaCl, 10 mM $MgCl_2$, 1 mM dithiotheitol, 0.1% Tween-20 and 200 μg ml^{-1} BSA. TopIB concentrations were between 0.5 and 20 nM. The rotation rate measurements were performed in identical buffer except that 2 mM $MgCl_2$ was used. The three nicking enzymes gave identical results, both in the step-size and the rotation rate measurements.

DNA constructs

Step-size measurements were performed with bacteriophage λ DNA molecules (48 kilobases (kb) or 16 μm contour length) that were coated at one extremity with multiple biotin groups and at the other with multiple digoxigenin groups. The rotation rate and the ΔLk distribution measurements at 0.2 pN were performed on half-length bacteriophage λ DNA molecules. In all molecules, the consensus sequence for vaccinia TopIB cleavage (5′-CCCTT↓, where ↓ denotes the cleavage site) appears frequently (63 times for the full-length λ DNA molecule). The DNA molecules were incubated with streptavidin-functionalized magnetic beads (1 μm diameter, Dynal) and introduced to the flow cell.

Magnetic tweezers/flow cell

The detailed experimental configuration of the magnetic tweezers, three-dimensional bead tracking, and force measurements have been described previously[19]. We measure F with 5% accuracy by continuously determining the three-dimensional bead position with 10 nm accuracy[19].

A custom-made flow cell was used, consisting of two rectangular glass microscope cover slides separated by a single layer of parafilm. The lower slide was coated with polystyrene and anti-digoxygenin. This surface was subsequently passivated with BSA.

Data analysis

For the step-size measurements, data traces were low-pass filtered at 2 Hz and averaged for >2 s, depending on force. Changes in DNA extension were analysed by making use of a sliding averaging window in which steps were accepted that were larger than three standard deviations of the Brownian noise of the bead[17]. The steps can be identified as arising from a single topoisomerase enzyme because the time it takes for the enzyme to remove supercoils is much smaller than the time between successive relaxation events. The bead velocity measurements were analysed from raw data obtained at 60 Hz.

Treatment of step-size distributions

Values for $\langle \Delta Lk \rangle$ were obtained using a modified maximum-likelihood method that takes into account the experimental bead noise and the fact that one cannot observe steps of $\Delta Lk > n$, where n is the number of supercoils in the DNA before cleavage. Therefore, the final step leading to the complete removal of plectonemes from the DNA is discarded. To correct for the ensuing overrepresentation of small steps, one takes into account that each measured step ΔLk_i is not drawn from the entire ΔLk distribution but rather from the probability distribution $P_i(\Delta Lk) = (N_i\langle \Delta Lk \rangle)^{-1}\exp(-\Delta Lk_i/\langle \Delta Lk \rangle)$, where N_i is given by $N_i = \exp(-\Delta Lk_{\mathrm{noise}}/\langle \Delta Lk \rangle) - \exp(\Delta Lk_{\mathrm{constrained},i}/\langle \Delta Lk \rangle)$, $\Delta Lk_{\mathrm{noise}}$ is the smallest observable step given the bead noise, and $\Delta Lk_{\mathrm{constrained},i}$ is the remaining number of supercoils in the DNA molecule before the ith step. The corresponding likelihood function L is thus given by: $L = \prod_{i=1}^{N}(N_i\langle \Delta Lk \rangle)^{-1}\exp(-\Delta Lk_i/\langle \Delta Lk \rangle)$. This modified maximum-likelihood method is especially useful at higher stretching forces, where failure to apply the method underestimates $\langle \Delta Lk \rangle$ by approximately 25%.

Received 11 November 2004; accepted 25 January 2005; doi:10.1038/nature03395.

1. Champoux, J. J. DNA topoisomerases: structure, function, and mechanism. *Annu. Rev. Biochem.* **70,** 369–413 (2001).
2. Corbett, K. D. & Berger, J. M. Structure, molecular mechanisms, and evolutionary relationships in DNA topoisomerases. *Annu. Rev. Biophys. Biomol. Struct.* **33,** 95–118 (2004).
3. Wang, J. C. DNA topoisomerases. *Annu. Rev. Biochem.* **65,** 635–692 (1996).
4. Liu, L. F. *et al.* Mechanism of action of camptothecin. *Ann. NY Acad. Sci.* **922,** 1–10 (2000).
5. Pommier, Y., Pourquier, P., Fan, Y. & Strumberg, D. Mechanism of action of eukaryotic DNA topoisomerase I and drugs targeted to the enzyme. *Biochim. Biophys. Acta* **1400,** 83–105 (1998).
6. Sekiguchi, J. & Shuman, S. Vaccinia topoisomerase binds circumferentially to DNA. *J. Biol. Chem.* **269,** 31731–31734 (1994).
7. Redinbo, M. R., Stewart, L., Kuhn, P., Champoux, J. J. & Hol, W. G. Crystal structures of human topoisomerase I in covalent and noncovalent complexes with DNA. *Science* **279,** 1504–1513 (1998).
8. Cheng, C., Kussie, P., Pavletich, N. & Shuman, S. Conservation of structure and mechanism between eukaryotic topoisomerase I and site-specific recombinases. *Cell* **92,** 841–850 (1998).
9. Kim, R. A. & Wang, J. C. Function of DNA topoisomerases as replication swivels in *Saccharomyces cerevisiae*. *J. Mol. Biol.* **208,** 257–267 (1989).
10. Stewart, L., Redinbo, M. R., Qiu, X., Hol, W. G. & Champoux, J. J. A model for the mechanism of human topoisomerase I. *Science* **279,** 1534–1541 (1998).
11. Stivers, J. T., Harris, T. K. & Mildvan, A. S. Vaccinia DNA topoisomerase I: evidence supporting a free rotation mechanism for DNA supercoil relaxation. *Biochemistry* **36,** 5212–5222 (1997).
12. Brown, P. O. & Cozzarelli, N. R. A sign inversion mechanism for enzymatic supercoiling of DNA. *Science* **206,** 1081–1083 (1979).
13. Brown, P. O. & Cozzarelli, N. R. Catenation and knotting of duplex DNA by type 1 topoisomerases: a mechanistic parallel with type 2 topoisomerases. *Proc. Natl Acad. Sci. USA* **78,** 843–847 (1981).
14. Brown, P. O., Peebles, C. L. & Cozzarelli, N. R. A topoisomerase from *Escherichia coli* related to DNA gyrase. *Proc. Natl Acad. Sci. USA* **76,** 6110–6114 (1979).
15. Liu, L. F., Liu, C. C. & Alberts, B. M. Type II DNA topoisomerases: enzymes that can unknot a topologically knotted DNA molecule via a reversible double-strand break. *Cell* **19,** 697–707 (1980).
16. Mizuuchi, K., Fisher, L. M., O'Dea, M. H. & Gellert, M. DNA gyrase action involves the introduction of transient double-strand breaks into DNA. *Proc. Natl Acad. Sci. USA* **77,** 1847–1851 (1980).
17. Dekker, N. H. *et al.* The mechanism of type IA topoisomerases. *Proc. Natl Acad. Sci. USA* **99,** 12126–12131 (2002).
18. Strick, T. R., Croquette, V. & Bensimon, D. Single-molecule analysis of DNA uncoiling by a type II topoisomerase. *Nature* **404,** 901–904 (2000).
19. Strick, T. R., Allemand, J. F., Bensimon, D., Bensimon, A. & Croquette, V. The elasticity of a single supercoiled DNA molecule. *Science* **271,** 1835–1837 (1996).
20. Rice, J. A. *Mathematical Statistics and Data Analysis* 31–59 (Wadsworth & Brooks/Cole Advanced Books & Software, Pacific Grove, 1988).
21. Shuman, S., Bear, D. G. & Sekiguchi, J. Intramolecular synapsis of duplex DNA by vaccinia topoisomerase. *EMBO J.* **16,** 6584–6589 (1997).
22. Sekiguchi, J. & Shuman, S. Requirements for noncovalent binding of vaccinia topoisomerase I to duplex DNA. *Nucleic Acids Res.* **22,** 5360–5365 (1994).
23. Sekiguchi, J. & Shuman, S. Identification of contacts between topoisomerase I and its target DNA by site-specific photocrosslinking. *EMBO J.* **15,** 3448–3457 (1996).
24. Carey, J. F., Schultz, S. J., Sisson, L., Fazzio, T. G. & Champoux, J. J. DNA relaxation by human topoisomerase I occurs in the closed clamp conformation of the protein. *Proc. Natl Acad. Sci. USA* **100,** 5640–5645 (2003).
25. Woo, M. H. *et al.* Locking the DNA topoisomerase I protein clamp inhibits DNA rotation and induces cell lethality. *Proc. Natl Acad. Sci. USA* **100,** 13767–13772 (2003).
26. Moroz, J. D. & Nelson, P. Torsional directed walks, entropic elasticity, and DNA twist stiffness. *Proc. Natl Acad. Sci. USA* **94,** 14418–14422 (1997).
27. Bustamante, C., Bryant, Z. & Smith, S. B. Ten years of tension: single-molecule DNA mechanics. *Nature* **421,** 423–427 (2003).
28. Krogh, B. O. & Shuman, S. DNA strand transfer catalyzed by vaccinia topoisomerase: peroxidolysis and hydroxylaminolysis of the covalent protein-DNA intermediate. *Biochemistry* **39,** 6422–6432 (2000).
29. Shuman, S., Golder, M. & Moss, B. Characterization of vaccinia virus DNA topoisomerase I expressed in *Escherichia coli*. *J. Biol. Chem.* **263,** 16401–16407 (1988).

Acknowledgements We thank P. Veenhuizen for help in constructing various DNA constructs, D. Bensimon, U. Keyser, R. Seidel, K. Neuman, L. Tian and B. Spanjaard for stimulating discussions, C. Wiggins for advice on statistical data analysis, D. Lubensky for discussions on polymer physics, and J. van der Does for machining of flow cells. We thank FOM and NWO for financial support.

Competing interests statement The authors declare that they have no competing financial interests.

Correspondence and requests for materials should be addressed to N.H.D. (nynke.dekker@mb.tn.tudelft.nl).